ORNL/TM-2000/200

SURFING: A Program for Precise Determination of Sample Position in Stress Measurements via Neutron Diffraction

D.-Q Wang[a], C. R. Hubbard[a] and X.-L. Wang[b]

[a]High Temperature Materials Lab

[b]Spallation Neutron Source

Oak Ridge National Laboratory

Oak Ridge, TN 37831-6064, USA

OAK RIDGE NATIONAL LABORATORY
U. S. DEPARTMENT OF ENERGY

UT-BATTELLE

SURFING: A program for precise determination of sample position in stress measurements via neutron diffraction

ABSTRACT

Precise determination of the specimen position relative to the sampling volume for texture and stress measurements by neutron diffraction is difficult or sometimes impossible using only optical devices due to large or irregular sample dimensions and/or complicated shape of the sampling volume. The knowledge of the shape and size of the sampling volume allows development of a general mathematical model for the intensity variation with a parallelogram-shape sampling volume moving from outside to inside the specimen for both transmission and reflection geometric set-ups. Both fixed slits and radial collimators are options in defining the geometrical setup. The attenuation by the sample also has been taken into account in this model. Experimental results agree well with the model calculations. The program SURFING is based on the model calculation and was written in Labwindows/CVI©.

1. INTRODUCTION

In a typical neutron diffraction experiment, the sampling volume is defined by slits inserted in the incident and diffracted beam paths near the specimen. In studies where the stress changes rapidly as a function of position, a small sampling volume and high position precision are required to reach the spatial resolution needed to accurately map the stress gradients. It is difficult or sometimes impossible to precisely determine specimen surface position using only theodolites and telescopes, due to large and irregular sample dimensions and/or complicated diffractometer layouts. The location of the sample surface with respect to the beam centerline can be obtained by observing the increase in intensity as the sampling volume enters the sample. This method has been used by a number of researchers for years [1-3]. It involves making a relatively quick scan, moving the sampling volume from a point off the surface to a point inside the sample. One then obtains a set of values of the integrated intensity versus position. A mathematical model then is fitted to the data to locate the sample surface position. Fitting models for the sampling volume with a rhombic prism and a rectangular section have been developed [2-3]. However, a more general shape of the sampling volume is a parallelogram, where the incident and diffraction beam width can be different. This report presents the general solution for both transmission and reflection set-ups and for use of a slit or radial collimator. The model calculations were validated with experiment results.

2. MODEL FOR THE CALCULATION OF INTENSITY VARIATION

The integrated neutron intensity during surface scanning is governed by two principal factors, absorption and scattering, though other phenomenon, such as multiple scattering, primary extinction, micro-absorption and texture [4] can also be involved in some circumstances. The integrated neutron intensity initially increases as the sampling volume enters the sample due to increasing diffracted volume. However, the attenuation by the sample also increases, and ultimately the measured intensity declines. The position where the integrated neutron intensity reaches a maximum depends on the shape of the sampling volume and the level of attenuation by the sample.

Taking into account the size of the sampling volume and the attenuation [2], the diffracted integrated intensity is given by:

$$I(x,y,z) = \int_{V_s} I_0(x,y,z)\exp(-\sigma l(x,y,z))dV \qquad (1)$$

where x, y, z are the coordinates of the sampling volume; I_0 is the incident neutron intensity; σ is the total attenuation coefficient; and l, the path length in the sample, is a function of the sampling volume size and position. The integration is performed over the sampling volume, V_S.

Two typical geometric setups, reflection and transmission, in stress measurement (Fig. 1) will be discussed below. Both cases are simplified by considering two-dimensional scans in the horizontal scattering plane and that the moving direction of the specimen is perpendicular to the sample surface.

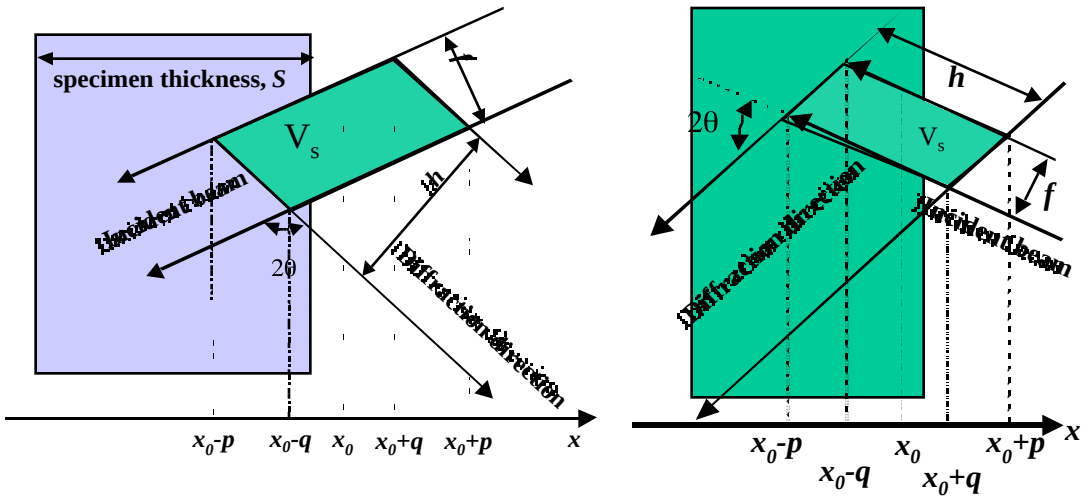

Fig. 1 Schematic drawing of the reflection (a), and transmission (b) geometric set-ups. The specimen surface to be located is perpendicular to x, and the specimen is translated parallel to the x-axis.

2.1 Reflection Set-up

This setup is for measurements of the strain component perpendicular to the sample surface, as shown in Fig. 1 (a). Generally, the sampling volume enters the specimen from one side and exits from the other side. The calculation of the integrated intensity is divided into nine regions. From Fig. 1 (a), one can obtain $p = \frac{h + f}{4\cos\theta}$, $q = \frac{h - f}{4\cos\theta}$, $h > f$, where h is the width of the diffracted beam; f is the width of the incident beam; 2θ is the diffraction angle; and x_0 is the position of the center of the sampling volume. The derivatives of the variables are calculated as the Levenberg-Marquardt method [5] implemented in the program SURFING needs the formulas.

In region I, where the sampling volume is outside of the sample, only the background, I_b, is detected.

$$I = I_b \qquad (2)$$

$$\frac{fI}{fx_0} = 0 \tag{3}$$

$$\frac{fI}{ff} = 0 \tag{4}$$

$$\frac{fI}{fh} = 0 \tag{5}$$

$$\frac{fI}{f\sigma} = 0 \tag{6}$$

In region II, $x_0 - p \le x \le x_0 - q$

$$I = \frac{I_0 \cos\theta}{\sigma}(x - x_0 + p) - \frac{I_0 \cos\theta \sin\theta}{2\sigma^2}\left[1 - \exp\left(-\frac{2\sigma}{\sin\theta}(x - x_0 + p)\right)\right] + I_b \tag{7}$$

$$\frac{fI}{fx_0} = \frac{I_0 \cos\theta}{\sigma}\left[\exp\left(-\frac{2\sigma}{\sin\theta}(x - x_0 + p)\right) - 1\right] \tag{8}$$

$$\frac{fI}{ff} = \frac{I_0}{4\sigma}\left[1 - \exp\left(-\frac{2\sigma}{\sin\theta}(x - x_0 + p)\right)\right] \tag{9}$$

$$\frac{fI}{fh} = \frac{fI}{ff} \tag{10}$$

$$\frac{fI}{f\sigma} = -\frac{I_0 \cos\theta}{\sigma^2}(x - x_0 + p)\left[1 + \exp\left(-\frac{2\sigma}{\sin\theta}(x - x_0 + p)\right)\right] + \frac{I_0 \cos\theta \sin\theta}{4\sigma^3}\left[1 - \exp\left(-\frac{2\sigma}{\sin\theta}(x - x_0 + p)\right)\right] \tag{11}$$

For region III, $x_0 - q \le x \le x_0 + q$ $(h \ge f)$

$$I = \frac{I_0 \cos\theta}{\sigma}\left[\frac{\sin\theta}{2\sigma}\exp\left(-\frac{2\sigma}{\sin\theta}(x - x_0 + p)\right) - \frac{\sin\theta}{2\sigma}\exp\left(-\frac{2\sigma}{\sin\theta}(x - x_0 + q)\right) + p - q\right] + I_b \tag{12}$$

$$\frac{fI}{fx_0} = \frac{I_0 \cos\theta}{\sigma}\left[\exp\left(-\frac{2\sigma}{\sin\theta}(x - x_0 + p)\right) - \exp\left(-\frac{2\sigma}{\sin\theta}(x - x_0 + q)\right)\right] \tag{13}$$

$$\frac{fI}{ff} = \frac{I_0}{4\sigma}\left[2 - \exp\left(-\frac{2\sigma}{\sin\theta}(x - x_0 + p)\right) - \exp\left(-\frac{2\sigma}{\sin\theta}(x - x_0 + q)\right)\right] \tag{14}$$

$$\frac{\partial I}{\partial h} = \frac{I_0}{4\sigma} \left[\exp\left(-\frac{2\sigma}{\sin\theta}(x - x_0 + q)\right) - \exp\left(-\frac{2\sigma}{\sin\theta}(x - x_0 + p)\right) \right] \tag{15}$$

$$\frac{\partial I}{\partial \sigma} = -\frac{I_0 \cos\theta}{\sigma^2}(x - x_0 + p) \left[\begin{array}{l} (x - x_0 + q + \frac{\sin\theta}{\sigma}) \exp\left(-\frac{2\sigma}{\sin\theta}(x - x_0 + q)\right) - p + q \\ -(x - x_0 + p + \frac{\sin\theta}{\sigma}) \exp\left(-\frac{2\sigma}{\sin\theta}(x - x_0 + p)\right) \end{array} \right] \tag{16}$$

In region IV $x_0 + q \le x \le x_0 + p$

$$I = \frac{I_0 \cos\theta}{\sigma} \left[\begin{array}{l} \frac{\sin\theta}{2\sigma} \exp\left(-\frac{2\sigma}{\sin\theta}(x - x_0 + p)\right) - \frac{\sin\theta}{2\sigma} \exp\left(-\frac{2\sigma}{\sin\theta}(x - x_0 + q)\right) \\ -\frac{\sin\theta}{2\sigma} \exp\left(-\frac{2\sigma}{\sin\theta}(x - x_0 - q)\right) + x_0 + p - x + \frac{\sin\theta}{2\sigma} \end{array} \right] + I_b \tag{17}$$

$$\frac{\partial I}{\partial x_0} = \frac{I_0 \cos\theta}{\sigma} \left[\begin{array}{l} \exp\left(-\frac{2\sigma}{\sin\theta}(x - x_0 + p)\right) - \exp\left(-\frac{2\sigma}{\sin\theta}(x - x_0 + q)\right) \\ -\exp\left(-\frac{2\sigma}{\sin\theta}(x - x_0 - q)\right) + 1 \end{array} \right] \tag{18}$$

$$\frac{\partial I}{\partial f} = \frac{I_0}{4\sigma} \left[\begin{array}{l} \exp\left(-\frac{2\sigma}{\sin\theta}(x - x_0 - q)\right) - \exp\left(-\frac{2\sigma}{\sin\theta}(x - x_0 + p)\right) \\ -\exp\left(-\frac{2\sigma}{\sin\theta}(x - x_0 + q)\right) + 1 \end{array} \right] \tag{19}$$

$$\frac{\partial I}{\partial h} = \frac{I_0}{4\sigma} \left[\begin{array}{l} \exp\left(-\frac{2\sigma}{\sin\theta}(x - x_0 + q)\right) - \exp\left(-\frac{2\sigma}{\sin\theta}(x - x_0 + p)\right) \\ -\exp\left(-\frac{2\sigma}{\sin\theta}(x - x_0 - q)\right) + 1 \end{array} \right] \tag{20}$$

$$\frac{\partial I}{\partial \sigma} = \frac{I_0 \cos\theta}{\sigma^2} \left[\begin{array}{l} (x - x_0 + q) \exp\left(-\frac{2\sigma}{\sin\theta}(x - x_0 + q)\right) + (x - x_0 - q) \exp\left(-\frac{2\sigma}{\sin\theta}(x - x_0 - q)\right) \\ -(x - x_0 + p) \exp\left(-\frac{2\sigma}{\sin\theta}(x - x_0 + p)\right) - x_0 - p + x \end{array} \right]$$

$$+ \frac{I_0 \cos\theta \sin\theta}{\sigma^3} \left[\exp\left(-\frac{2\sigma}{\sin\theta}(x - x_0 + q)\right) + \exp\left(-\frac{2\sigma}{\sin\theta}(x - x_0 - q)\right) - \exp\left(-\frac{2\sigma}{\sin\theta}(x - x_0 - p)\right) - 1 \right] \tag{21}$$

In region V, $x_0 + p \le x \le S + x_0 - p$

$$I = \frac{I_0 \sin\theta \cos\theta}{2\sigma^2} \left[\exp\left(-\frac{2\sigma}{\sin\theta}(x - x_0 + p)\right) - \exp\left(-\frac{2\sigma}{\sin\theta}(x - x_0 + q)\right) + \exp\left(-\frac{2\sigma}{\sin\theta}(x - x_0 - p)\right) - \exp\left(-\frac{2\sigma}{\sin\theta}(x - x_0 - q)\right) \right] + I_b \quad (22)$$

$$\frac{\partial I}{\partial x_0} = \frac{I_0 \cos\theta}{\sigma} \left[\exp\left(-\frac{2\sigma}{\sin\theta}(x - x_0 + p)\right) - \exp\left(-\frac{2\sigma}{\sin\theta}(x - x_0 + q)\right) - \exp\left(-\frac{2\sigma}{\sin\theta}(x - x_0 - p)\right) - \exp\left(-\frac{2\sigma}{\sin\theta}(x - x_0 - q)\right) \right] \quad (23)$$

$$\frac{\partial I}{\partial \theta} = \frac{I_0}{4\sigma} \left[\exp\left(-\frac{2\sigma}{\sin\theta}(x - x_0 - p)\right) - \exp\left(-\frac{2\sigma}{\sin\theta}(x - x_0 + q)\right) + \exp\left(-\frac{2\sigma}{\sin\theta}(x - x_0 - q)\right) - \exp\left(-\frac{2\sigma}{\sin\theta}(x - x_0 + p)\right) \right] \quad (24)$$

$$\frac{\partial I}{\partial h} = \frac{I_0}{4\sigma} \left[\exp\left(-\frac{2\sigma}{\sin\theta}(x - x_0 - p)\right) - \exp\left(-\frac{2\sigma}{\sin\theta}(x - x_0 - q)\right) + \exp\left(-\frac{2\sigma}{\sin\theta}(x - x_0 + q)\right) - \exp\left(-\frac{2\sigma}{\sin\theta}(x - x_0 + p)\right) \right] \quad (25)$$

$$\frac{\partial I}{\partial \sigma} = \frac{I_0 \cos\theta}{\sigma^2} \left[(x - x_0 + q)\exp\left(-\frac{2\sigma}{\sin\theta}(x - x_0 + q)\right) + (x - x_0 - q)\exp\left(-\frac{2\sigma}{\sin\theta}(x - x_0 - q)\right) - (x - x_0 + p)\exp\left(-\frac{2\sigma}{\sin\theta}(x - x_0 + p)\right) - (x - x_0 - p)\exp\left(-\frac{2\sigma}{\sin\theta}(x - x_0 - p)\right) \right] + \frac{I_0 \cos\theta \sin\theta}{2\sigma^3} \left[\exp\left(-\frac{2\sigma}{\sin\theta}(x - x_0 + q)\right) + \exp\left(-\frac{2\sigma}{\sin\theta}(x - x_0 - q)\right) - \exp\left(-\frac{2\sigma}{\sin\theta}(x - x_0 - p)\right) - \exp\left(-\frac{2\sigma}{\sin\theta}(x - x_0 + p)\right) \right] \quad (26)$$

In region VI, $S - p + x_0 \le x \le S + x_0 - q$

$$I = \frac{I_0 \cos\theta}{\sigma} \left[\frac{\sin\theta}{2\sigma} \exp\left(-\frac{2\sigma}{\sin\theta}(x - x_0 - p)\right) - \frac{\sin\theta}{2\sigma} \exp\left(-\frac{2\sigma}{\sin\theta}(x - x_0 + q)\right) - \frac{\sin\theta}{2\sigma} \exp\left(-\frac{2\sigma}{\sin\theta}(x - x_0 - q)\right) + \left(\frac{\sin\theta}{2\sigma} + s + x_0 - x - p\right)\exp\left(-\frac{2\sigma S}{\sin\theta}\right) \right] + I_b \quad (27)$$

$$\frac{fI}{fx_0} = \frac{I_0 \cos\theta}{\sigma} \begin{matrix} \exp\left(-\frac{2\sigma S}{\sin\theta}\right) - \exp\left(-\frac{2\sigma}{\sin\theta}(x - x_0 + q)\right) \\ \exp\left(-\frac{2\sigma}{\sin\theta}(x - x_0 - p)\right) - \exp\left(-\frac{2\sigma}{\sin\theta}(x - x_0 - q)\right) \end{matrix} \quad (28)$$

$$\frac{fI}{ff} = \frac{I_0}{4\sigma} \begin{matrix} \exp\left(-\frac{2\sigma}{\sin\theta}(x - x_0 - p)\right) - \exp\left(-\frac{2\sigma}{\sin\theta}(x - x_0 + q)\right) \\ + \exp\left(-\frac{2\sigma}{\sin\theta}(x - x_0 - q)\right) - \exp\left(-\frac{2\sigma S}{\sin\theta}\right) \end{matrix} \quad (29)$$

$$\frac{fI}{fh} = \frac{I_0}{4\sigma} \begin{matrix} \exp\left(-\frac{2\sigma}{\sin\theta}(x - x_0 - p)\right) + \exp\left(-\frac{2\sigma}{\sin\theta}(x - x_0 + q)\right) \\ - \exp\left(-\frac{2\sigma}{\sin\theta}(x - x_0 - q)\right) - \exp\left(-\frac{2\sigma S}{\sin\theta}\right) \end{matrix} \quad (30)$$

$$\frac{fI}{f\sigma} = \frac{I_0 \cos\theta}{\sigma^2} \begin{matrix} (x - x_0 + q)\exp\left(-\frac{2\sigma}{\sin\theta}(x - x_0 + q)\right) + (x - x_0 - q)\exp\left(-\frac{2\sigma}{\sin\theta}(x - x_0 - q)\right) \\ -(x - x_0 + p)\exp\left(-\frac{2\sigma}{\sin\theta}(x - x_0 + p)\right) - (2S - x + x_0 - p)\exp\left(-\frac{2\sigma S}{\sin\theta}\right) \end{matrix}$$

$$+ \frac{I_0 \cos\theta \sin\theta}{\sigma^3} \begin{matrix} \exp\left(-\frac{2\sigma}{\sin\theta}(x - x_0 + q)\right) + \exp\left(-\frac{2\sigma}{\sin\theta}(x - x_0 - q)\right) \\ -\exp\left(-\frac{2\sigma}{\sin\theta}(x - x_0 - p)\right) - \exp\left(-\frac{2\sigma S}{\sin\theta}\right) \end{matrix}$$

$$- \frac{2I_0 S \cos\theta}{\sigma \sin\theta}(S + x_0 - x - p)\exp\left(-\frac{2\sigma S}{\sin\theta}\right) \quad (31)$$

$$\frac{fI}{fS} = \frac{I_0 \cos\theta}{\sigma} \left[2 + \frac{2\sigma}{\sin\theta}(S + x_0 - x - p)\right] \exp\left(-\frac{2\sigma S}{\sin\theta}\right) \quad (32)$$

For region VII, $S + x_0 - q \le x \le S + x_0 + q$

$$I = \frac{I_0 \cos\theta}{\sigma} \begin{matrix} \frac{\sin\theta}{2\sigma} \exp\left(-\frac{2\sigma}{\sin\theta}(x - x_0 - p)\right) - \frac{\sin\theta}{2\sigma} \exp\left(-\frac{2\sigma}{\sin\theta}(x - x_0 - q)\right) \\ -(p - q)\exp\left(-\frac{2\sigma S}{\sin\theta}\right) \end{matrix} + I_b \quad (33)$$

$$\frac{fI}{fx_0} = \frac{I_0 \cos\theta}{\sigma} \left[\exp\left(-\frac{2\sigma}{\sin\theta}(x - x_0 - p)\right) - \exp\left(-\frac{2\sigma}{\sin\theta}(x - x_0 - q)\right) \right] \quad (34)$$

$$\frac{fI}{ff} = \frac{I_0}{4\sigma} \left[\exp\left(-\frac{2\sigma}{\sin\theta}(x - x_0 - p)\right) + \exp\left(-\frac{2\sigma}{\sin\theta}(x - x_0 - q)\right) - 2\exp\left(-\frac{2\sigma S}{\sin\theta}\right) \right] \quad (35)$$

$$\frac{fI}{fh} = \frac{I_0}{4\sigma} \left[\exp\left(-\frac{2\sigma}{\sin\theta}(x - x_0 - p)\right) - \exp\left(-\frac{2\sigma}{\sin\theta}(x - x_0 - q)\right) \right] \quad (36)$$

$$\frac{fI}{f\sigma} = \frac{I_0 \cos\theta}{\sigma^2} \left[\begin{array}{l} (x - x_0 - q)\exp\left(-\frac{2\sigma}{\sin\theta}(x - x_0 - q)\right) \\ -(x - x_0 - p)\exp\left(-\frac{2\sigma}{\sin\theta}(x - x_0 - p)\right) + (p - q)\exp\left(-\frac{2\sigma S}{\sin\theta}\right) \end{array} \right]$$

$$+ \frac{I_0 \cos\theta \sin\theta}{\sigma^3} \left[\exp\left(-\frac{2\sigma}{\sin\theta}(x - x_0 - q)\right) - \exp\left(-\frac{2\sigma}{\sin\theta}(x - x_0 - p)\right) \right] - \frac{2I_0 S \cos\theta}{\sigma \sin\theta}(p - q)\exp\left(-\frac{2\sigma S}{\sin\theta}\right) \quad (37)$$

$$\frac{fI}{fS} = \frac{2I_0 \cos\theta}{\sin\theta}(p - q)\exp\left(-\frac{2\sigma S}{\sin\theta}\right) \quad (38)$$

In region VIII, $S + x_0 + q \le x \le S + x_0 + p$

$$I = \frac{I_0 \cos\theta}{\sigma} \left[\frac{\sin\theta}{2\sigma} \exp\left(-\frac{2\sigma}{\sin\theta}(x - x_0 - p)\right) - \left(\frac{\sin\theta}{2\sigma} + s + x_0 + p - x\right)\exp\left(-\frac{2\sigma S}{\sin\theta}\right) \right] + I_b \quad (39)$$

$$\frac{fI}{fx_0} = \frac{I_0 \cos\theta}{\sigma} \left[\exp\left(-\frac{2\sigma}{\sin\theta}(x - x_0 - p)\right) - \exp\left(-\frac{2\sigma S}{\sin\theta}\right) \right] \quad (40)$$

$$\frac{fI}{ff} = \frac{I_0}{4\sigma} \left[\exp\left(-\frac{2\sigma}{\sin\theta}(x - x_0 - p)\right) - \exp\left(-\frac{2\sigma S}{\sin\theta}\right) \right] \quad (41)$$

$$\frac{fI}{fh} = \frac{fI}{ff} \quad (42)$$

$$\frac{fI}{f\sigma} = \frac{I_0 \cos\theta}{\sigma^2}\left[(S + x_0 + p - x)\exp\left(-\frac{2\sigma S}{\sin\theta}\right) - (x - x_0 - p)\exp\left(-\frac{2\sigma}{\sin\theta}(x - x_0 - p)\right)\right]$$
$$+\frac{I_0 \cos\theta \sin\theta}{\sigma^3}\left[\exp\left(-\frac{2\sigma S}{\sin\theta}\right) - \exp\left(-\frac{2\sigma}{\sin\theta}(x - x_0 - p)\right)\right]$$
$$+\frac{2I_0 S\cos\theta}{\sigma \sin\theta}\left(\frac{\sin\theta}{2\sigma} + S + x_0 + p - x\right)\exp\left(-\frac{2\sigma S}{\sin\theta}\right) \tag{43}$$

$$\frac{fI}{fS} = \frac{2I_0 \cos\theta}{\sin\theta}(S + x_0 + p - x)\exp\left(-\frac{2\sigma S}{\sin\theta}\right) \tag{44}$$

In region IX, $S + x_0 + p \le x$, where the sampling volume moves outside of the back surface of the sample, again only the background is detected.

$$I = I_b \tag{45}$$

2.2 Transmission Set-up

This set-up is particularly used for in-plane strain measurements, as shown in Fig. 1(b). The change of the diffraction intensity only comes from variation of the diffracted volume since the path length, *l*, in the sample is always the same when the sampling volume moves through the sample surface along the direction perpendicular to the sample surface. Five regions are considered in the calculation.

From Fig. 1 (b), one can obtain $p = \frac{h + f}{4\sin\theta}$, $q = \frac{h - f}{4\sin\theta}$, $(h > f)$

In region I, $x \le x_0 - p$,

$$I = I_b \tag{46}$$

In region II, $x_0 - p \le x \le x_0 - q$,

$$I = I_0 \tan\theta \left[x - (x_0 - p)\right]^2 + I_b \tag{47}$$

$$\frac{fI}{fx_0} = -2I_0 \tan\theta\,(x - x_0 + p) \tag{48}$$

$$\frac{fI}{ff} = \frac{I_0}{2\cos\theta}(x - x_0 + p) \tag{49}$$

$$\frac{fI}{fh} = \frac{fI}{ff} \tag{50}$$

In region III, $x_0 - q \le x \le x_0 + q$,

$$I = I_0 \ (p - q)^2 \tan\theta + \frac{f}{\cos\theta}(x - x_0 + q) + I_b \tag{51}$$

$$\frac{fI}{fx_0} = -\frac{fI_0}{\cos\theta} \tag{52}$$

$$\frac{fI}{ff} = \frac{I_0}{\cos\theta}(x - x_0 + p - \frac{f}{4\cos\theta}) \tag{53}$$

$$\frac{fI}{fh} = \frac{fI_0}{4\sin\theta\cos\theta} \tag{54}$$

In region IV, $x_0 + q \le x \le x_0 + p$,

$$I = I_0 \tan\theta\left[2(p-q)^2 - (x_0 + p - x)^2\right] + \frac{2fq}{\cos\theta} + I_b \tag{55}$$

$$\frac{fI}{fx_0} = 2I_0\tan\theta\,(x - x_0 - p) \tag{56}$$

$$\frac{fI}{ff} = \frac{I_0}{2\cos\theta}(3p - x - x_0 - \frac{f}{\sin\theta}) \tag{57}$$

$$\frac{fI}{fh} = \frac{I_0}{2\cos\theta}(x - x_0 - P + \frac{f}{\sin\theta}) \tag{58}$$

In region V, $x_0 + p \le x$

$$I = I_0[2\tan\theta\,(p-q)^2 + \frac{2fq}{\cos\theta}] + I_b \tag{59}$$

$$\frac{fI}{fx_0} = 0 \tag{60}$$

$$\frac{fI}{ff} = \frac{I_0}{\cos\theta}(2p - \frac{f}{2\sin\theta}) \tag{61}$$

$$\frac{fI}{fh} = \frac{fI_0}{2\cos\theta i\sin\theta} \tag{62}$$

An assumption was made in the model that the spatial distribution of the intensity of both the incident, $I_0(x, y, z)$, and diffracted, $I(x, y, z)$, beams are "square pulses", i.e. the incident intensity is distributed uniformly within the region defined by the slits and zero outside. This is not quite correct in reality because of beam divergence. The incident beam

divergence is largely determined by the characteristics of the monochromator/moderator and optical devices in the incident beam path [6-8] whilst the optical devices in the diffracted beam path and attenuation by the sample influence the diffracted beam divergence [4]. The effect of a non-square-pulse distribution of beam intensity is modeled by an effective beam width, the full-width-at-half-maximum (FWHM) of the intensity [3] in our calculations. The size of the effective beam width relies on both the beam divergence and the distance between the center of the sampling volume and the slit.

3. VALIDATION OF THE CALCULATION MODELS

3.1 Comparison with more limited models

The previous models for the sampling volume with a rhombic prism and a rectangular section [2-3] can be derived from this calculation. If h = f, the section of the sampling volume possesses a rhombic prism shape, $p = \frac{h}{2\cos\theta}, q = 0$. Equations (2, 7, 12, 17, 22, 27, 33, 39) become the equations in reference [2] except that the scan for the backside surface of the specimen in the reflection geometry was ignored. If $\theta = 45°$, the section of the sampling volume is a rectangle, $p = \frac{h+f}{2\sqrt{2}}, q = \frac{h-f}{2\sqrt{2}}, h ? f$. Equations (2, 7, 12, 17, 22, 27, 33, 39) are simplified to the cases in reference [3].

3.2 Comparison with experimental results

Experiments were carried out at HB2 of HFIR, Oak Ridge National Lab. A detector array consisting of seven ORDELA position-sensitive detectors distributed along a vertical arc at equal distance to the same position was used for data acquisition. The angular acceptance in

the scattering plane for each detector is approximately six degrees in 2θ. The detectors are separated vertically by seven degrees with the central detector situated in the horizontal scattering plane. The integrated intensity used was the sum of the intensities from the seven detectors. A rectangular stainless steel plate (10x50x50 mm^3) was used for the validation. The incident slit size was 1 mm wide and 4 mm high, located 50 mm from the rotation center of the positioner. In order to test the model, large differences of the widths between the incident and receiving slit were used. Thus a 2.5-mm-wide receiving slit was placed at 40 mm away from the rotation center of the positioner. The wavelength of the incident neutron beam was 1.65 Å. For the reflection geometric setup, the (222) reflection of stainless steel was used at 105° (2θ). The results of the measurement are shown in Fig. 2. The measurement errors for the intensity were small, as a relatively long counting time was used for every point (1.6 minutes per step). The fitting method was a standard Levenberg-Marquardt least-square fitting routine [5]. As can be seen, the experimental data fit well with the model. The measured thickness of the stainless steel plate determined by the fitting method, *S*, was 9.93 mm, which is 0.07 mm smaller than the thickness measured by a caliper.

For the transmission setup, the (220) reflection was used and the diffraction angle (2θ) was 81°. Fig. 3 shows the comparison of the experimental data with the model calculation. A good agreement was also observed, though the measurement errors were larger than those in Fig. 2 due to faster scan (0.2 minutes per step).

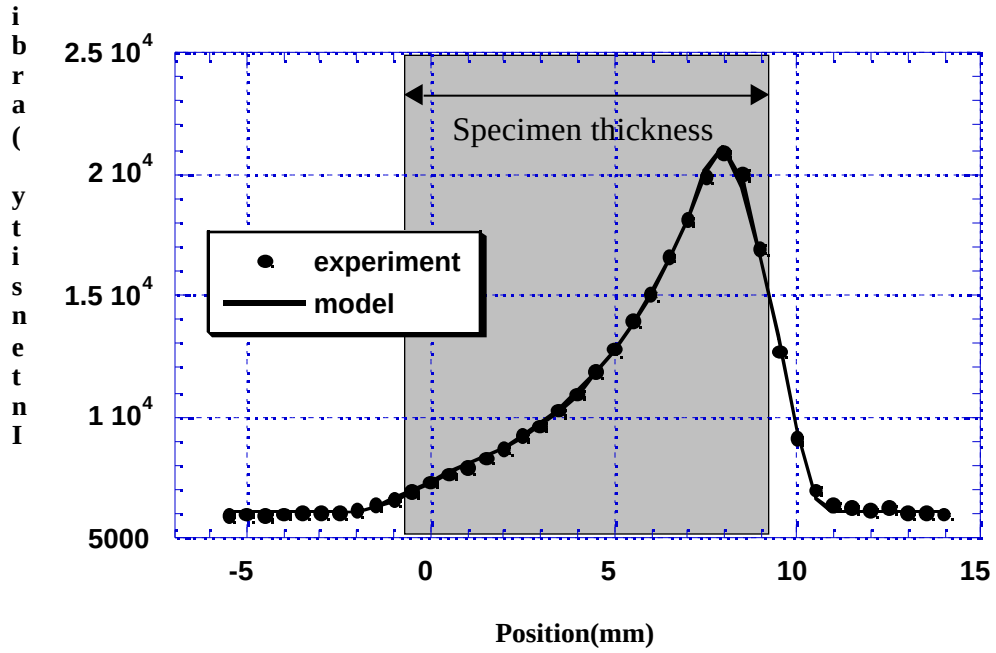

Fig. 2 Comparison of model calculations and experimental results for a steel plate. The incident slit size was 1 mm wide and 4 mm high. The width of the receiving slit was 2.5 mm. The diffraction angle (2θ) was 105°. The measurement errors of the intensity are smaller than the black symbols.

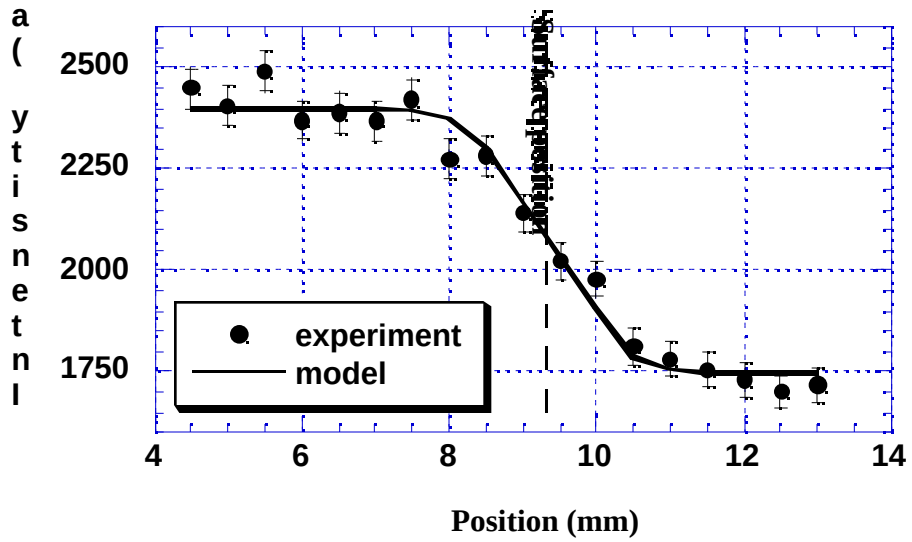

Fig. 3 Comparison of the modeling calculations and the experimental results for transmission geometric setup with (220) reflection of an iron plate. The slit sizes were the same as those in the experiment with the reflection geometry setup. The diffraction angle (2θ) was 81°.

4. Using the program SURFING

4.1 Installation

The program runs on either a Windows 95/98 or NT (V 4.0 or higher) workstation. The program installation kit can be obtained by email (make inquiry to wangdq@ornl.gov). Please make sure to put all files in the same folder. Double click on the SETUP.EXE program, then follow the instruction on the screen to complete installation.

4.2 Input and output

After installing the program you are ready to run it by just clicking the SURFING icon. The graphic interface is shown in Fig. 4. There is a help button in the menu bar. One can have general instruction about the program by clicking on the "Help". The Levenberg-Marquardt method [5] is implemented in the program. The following is a step-by-step instruction set for the program.

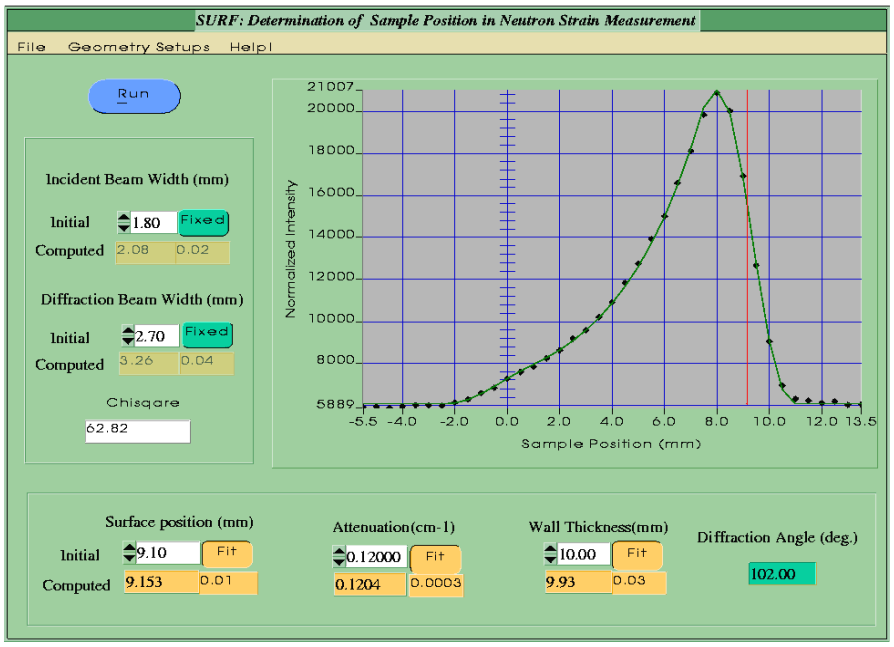

Fig. 4 The graphic window of the program.

Step 1: Open a file with measurement data

Click on File-Open on the menu bar, when one can load a text file with the values of two-theta angle, positions and intensities, which has a format as shown below:

102 (two-theta angle)

(position in mm)	(intensity)
20.3	150

20.8	200
21.3	300
21.8	350
...	...

Note that the text in the brackets should not be included in the text file.

Step 2: Choose the parameters to be fitted

Next step is to choose the geometry setup from the menu bar. There are three types of geometry setup: transmission, reflection and wall-scan. Note that the geometry setup "wall-scan" is basically the same as the "reflection" except that it covers a full range through the thickness of a plate in the reflection geometry setup. The input parameters are listed in Table 1. One can make the choice whether he wants to fit the parameter or not by clicking on the button, “Fit/Fixed” on the same line with the word “initial”. If a parameter is fixed, the numerical window in the same line with the word “computed” is dimmed.

Step 3: Run the fitting procedure

After clicking on the button “Run”, the numerical windows in the line with the word “computed” will show the fitted value (left) and the standard deviation (right). Note that the least-square fitting routine may crash if the initial values of the parameters are far off from their "real" values. In the case of “Wall-Scan”, the initial value of the surface position should be the front surface’s, e.g., the surface position closest to that of the maximum intensity.

Table 1. List of the Input parameters

	Transmission	Reflection	Wall-scan
Incident beam width (mm)	√	√	√

Diffracted beam width (mm)	√	√	√
Sample position (mm)	√	√	√
Attenuation coefficient (mm^{-1})	×	√	√
Wall thickness (mm)	×	×	√
Two-theta angle (degrees)	*	*	*

√: the parameter can be fitted.

×: the parameter is not a variable for the geometry setup.

*: the parameter is fixed.

Step 4: Save the fitted data and print the graphic window

After running the "fit" procedure, one can also save the fitted parameters and curve values in a text file by clicking on "File-Save" in the menu bar. It is also possible for the user to print out the graphic window using "File-Print" in the menu bar.

5. Conclusions

A generic model calculation of the intensity variation with a sampling volume moving from off to inside a sample surface for both reflection and transmission setups was developed for use in stress measurement with neutron diffraction. Experiments for scans performed on a stainless steel plate at two different scattering angles show that the model calculation agrees well with the experiment result. A program, SURFING, based on the model, was developed and can be run on Windows95/98 or NT systems.

Acknowledgement

Research sponsored by the Assistant Secretary for Energy Efficiency and Renewable Energy, Office of Transportation Technologies, as part of the High Temperature Materials Laboratory User Program, Oak Ridge National Laboratory, managed by UT-Battelle, LLC, for the U.S. Dept. of Energy under contract DE-AC05-00OR22725**.** We also thank Dr. Ru Lin Peng for providing the specimen. DQW was supported in part by an appointment to the Oak Ridge National Laboratory Postdoctoral Research Associates Program administrated jointly by the Oak Ridge National Laboratory and the Oak Ridge Institute for Science and Education.

Reference

1 Ezeilo A.N., "Residual stress determinations by neutron and X-ray diffraction methods", *Ph.D. thesis*, Imperial College, University of London, 1992

2 Brand P.C. and Prask H.J., “New methods for the alignment of instrumentation for residual-stress measurements by means of neutron diffraction”, *J. Appl. Cryst.* 27(1994)164

3 Wang D. Q., and Edwards L., “Precise determination of specimen surface position during sub-surface strain scanning by neutron diffraction”, Proc. of Fourth European Conference on Residual Stresses, p135-143, France 1996

4 Bacon G. E., *Neutron Diffraction* (Clarendon Press, Oxford, 1962), Chap. 2 & 3

5 Press W.H., Teukolsky S.A, Vetterling W.T. and Flannery B.P., (Cambridge University Press, 1992), *Numerical Recipes in C*, Chapter 15

6 Copley, J. R. D., "Transmission properties of short curved neutron guides: Part I. Acceptance diagram analysis and calculations", Nuclear Instruments & Methods in Phyiscs Research A 355(1995)469-477

7 Wang, D.-Q, Robertson, R. L., Crow L., Wang, X.-L, and Lee W.-T., "Modeling neutron guides by Monte Carlo Simulation", in preparation.

8 Popovici, M. and Yelon, W. B., "A high performance focusing silicon monochromator", *J. Neutron Research*, Vol. 5, pp227-239.